Original Article

Age-related focal thinning of the ganglion cell-inner plexiform layer in a healthy population

Yuqing Deng[1,2#], Huijuan Wang[2,3#], Ava-Gaye Simms[2], Huiling Hu[2,4], Juan Zhang[2,5], Giovana Rosa Gameiro[2], Tatjana Rundek[6], Joseph F. Signorile[7,8], Bonnie E. Levin[6], Jin Yuan[1,2], Jianhua Wang[2], Hong Jiang[2,6]

[1]State Key Laboratory of Ophthalmology, Zhongshan Ophthalmic Center, Sun Yat-sen University, Guangzhou, China; [2]Department of Ophthalmology, Bascom Palmer Eye Institute, University of Miami Miller School of Medicine, Miami, FL, USA; [3]Eye Hospital, China Academy of Chinese Medical Sciences, Beijing, China; [4]Shenzhen Key Laboratory of Ophthalmology, Shenzhen Eye Hospital, Jinan University, Shenzhen, China; [5]School of Ophthalmology and Optometry, School of Biomedical Engieering, Wenzhou Medical University, Wenzhou, China; [6]Department of Neurology, The Evelyn F. McKnight Brain Institute, University of Miami Miller School of Medicine, Miami, FL, USA; [7]Max Orovitz Laboratory, University of Miami, Coral Gables, FL, USA; [8]Center on Aging, University of Miami, School of Medicine, Miami, FL, USA

Contributions: (I) Conception and design: J Wang, J Yuan; (II) Administrative support: H Jiang, J Wang; (III) Provision of study materials or patients: T Rundek, JF Signorile, BE Levin; (IV) Collection and assembly of data: Y Deng, H Wang; (V) Data analysis and interpretation: Y Deng, H Wang, AG Simms, H Hu, J Zhang, GR Gameiro; (VI) Manuscript writing: All authors; (VII) Final approval of manuscript: All authors.

[#]These authors contributed equally to this work and should be considered as co-first authors.

Correspondence to: Jianhua Wang. Department of Ophthalmology, Bascom Palmer Eye Institute, University of Miami Miller School of Medicine, Miami, FL 33136, USA. Email: jwang3@med.miami.edu.

Background: Given the aging of the population worldwide, to learn the underlying age-related biological phenomena is important to improve the understanding of the ageing process. Neurodegeneration is an age-associated progressive deterioration of the neuron. Retinal neurodegeneration during aging, such as the reduction in thickness of the retinal nerve fiber layer (RNFL) and ganglion cell-inner plexiform layer (GCIPL) measured by optical coherence tomography (OCT), has been reported, but no studies have provided their specific alteration patterns with age. Therefore, this study is to provide visualization of the evolution of various tomographic intraretinal layer thicknesses during aging and to document age-related changes in focal thickness.

Methods: A total 194 healthy subjects were included in this cross-sectional study. The subjects were divided into four age groups: G1, <35 years; G2, 35–49 years; G3, 50–64 years; and G4 ≥65 years. One eye of each subject was imaged using a custom-built ultrahigh-resolution optical coherence tomography (UHR-OCT). Volumetric data centered on the fovea were segmented to obtain the thickness maps of six intraretinal layers, including the macular retinal nerve fiber layer (mRNFL) and GCIPL.

Results: There were alterations visualized in thickness maps in these intraretinal layers. The GCIPL showed a thickness reduction localized in the inner annulus in elder subjects (G4). Within the inner annulus, the most profound alteration in G4, an oval zone (length 0.76 mm and width 0.52 mm), appeared to be in the inferior sector about 0.61 mm below the fovea, named "A zone". The average thickness reduction of the A zone was 14.4 μm in the elderly group (G4). Age was significantly related to the GCIPL thickness of the inner annulus (ρ =–0.48; P<0.001) and of the A zone (ρ =–0.39, P<0.001).

Conclusions: This is the first study to apply UHR-OCT for visualizing the age-related alteration of intraretinal layers in a general population. The most profound change of the optic nerve fiber is an oval-like focal thinning in GCIPL, which occurred in the inferior sector within the inner annulus and was strongly related to increased age.

Keywords: Aging; focal thinning; ganglion cell-inner plexiform layer (GCIPL); ultrahigh-resolution optical coherence tomography (UHR-OCT)

Submitted Sep 09, 2021. Accepted for publication Mar 11, 2022.
doi: 10.21037/qims-21-860
View this article at: https://dx.doi.org/10.21037/qims-21-860

Introduction

Neurodegeneration is an age-associated progressive deterioration of neuronal structures and functions, which may lead to cognitive impairment and affect lifespan potentials (1). Morphological alterations, such as axonal swelling, microtubule disassembly, and nerve cell body loss, are characteristic features in many neurodegenerative conditions (2). The retina is an extension of the brain and provides a unique opportunity for studying the effect of aging on the central nervous system. It provides an opportunity to study both physiological and pathophysiological mechanisms related to aging (3,4). Retinal neurodegeneration during aging, such as the reduction in thickness of the retinal nerve fiber layer (RNFL) and ganglion cell-inner plexiform layer (GCIPL) measured by optical coherence tomography (OCT), has been reported (3-10). Based on the average thickness of the neuronal layers, including RNFL and GCIPL, previous studies have documented that age plays a role in retinal neurodegeneration (6-8,10). Also, previous studies showed uneven alterations (sectorial thinning) of the GCIPL due to aging (6-10). The majority of the studies differentiated sectorial thinning by commonly used partitions including the early treatment of diabetic retinopathy study (ETDRS) (8) and Zeiss elliptical partition (6,7). Only one study provided visualization of the tomographic thickness pattern of GCIPL averaged from a group of healthy subjects, and it demonstrated thinner GCIPL in the inferior sector (10). However, no studies have provided visualization of the evolution of various tomographic intraretinal layer thicknesses during aging. The aim of the present study is to provide visualization of the evolution of various tomographic intraretinal layer thicknesses during aging and to document age-related changes in focal thickness. We present the following article in accordance with the STROBE reporting checklist (available at https://qims.amegroups.com/article/view/10.21037/qims-21-860/rc).

Methods

Participants

A total 194 healthy subjects were included in this cross-sectional study between January 1, 2016, and December 31, 2020. The study was conducted in accordance with the Declaration of Helsinki (as revised in 2013) and approved by the Institutional Review Board of the University of Miami Miller School of Medicine. An informed consent form was signed by each subject. The subjects with severe media opacity, such as severe cataract and vitreous opacity were excluded. The subjects were also excluded if they had a refractive error greater than ±6 diopters.

The subjects were divided into four age groups, based on previous research in this area (5,11). Group 1 (G1) included subjects <35 years of age, Group 2 (G2) 35 to 49 years, Group 3 (G3) 50 to 64 years, and Group 4 (G4) included subjects 65 years of age or older. All subjects underwent detailed ophthalmic examinations such as best-corrected visual acuity, manifest refraction, and slit-lamp examination.

Intraretinal tomographic thicknesses using ultrahigh-resolution optical coherence tomography (UHR-OCT)

The custom-built UHR-OCT device used in the study was described previously (5,11-14). Briefly, this system is a spectral-domain OCT with an axial resolution of ~3 μm (in tissue) and a scan speed of 24,000 A-scans per second. In the present study, the macula was scanned using a 512 A-scans × 128 B-scans cube scan protocol, covering an area of 6×6 mm centered on the fovea. One eye of each subject was imaged. The right eye was the first choice for imaging. If the right eye was not eligible, the left eye was imaged. The volumetric dataset was exported and segmented into six intra-retinal layers using a commercially available software program (Orion, Voxeleron LLC, Pleasanton, CA, USA) (5,11,12,14) (*Figure 1*). To verify the segmentation of the dataset, segmentation of all intraretinal

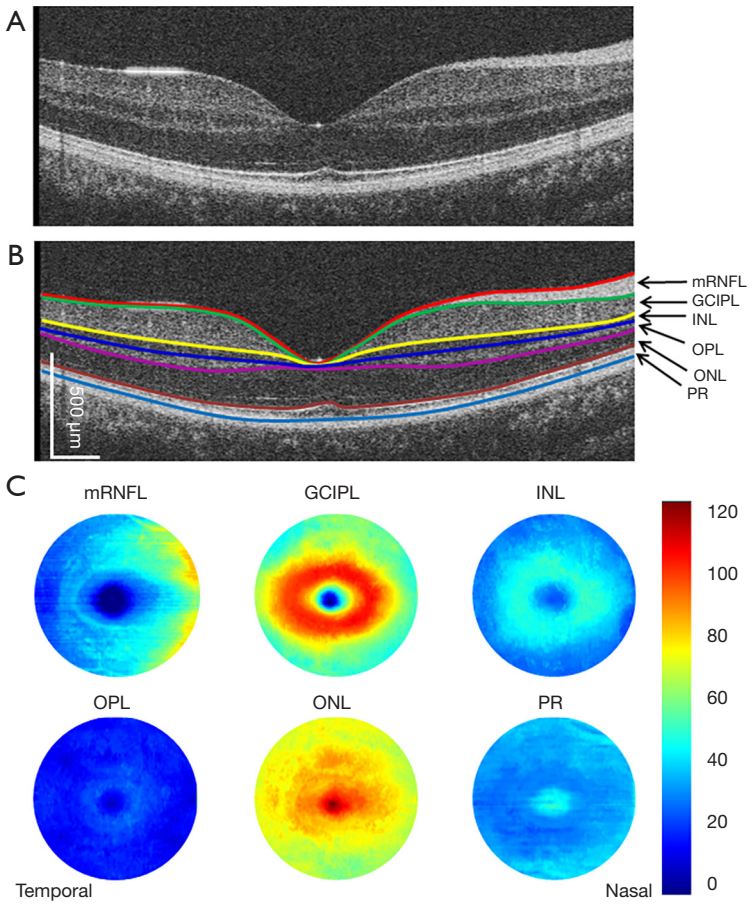

Figure 1 Cross-sectional retina and segmented tomographic thickness maps of intraretinal layers. The retina (A) of a healthy subject was scanned using UHR-OCT and 6 intraretinal layers (B) were segmented using the Orion software. There are seven segmented boundaries, defining six intraretinal layers, which correspond to six tomographic thickness maps (C, diameter of 6 mm). RNFL, retinal nerve fiber layer; GCIPL, ganglion cell-inner plexiform layer; INL, inner nuclear layer; OPL, outer plexiform layer; ONL, outer nuclear layer; PR, retinal photoreceptor; mRNFL, macular retinal nerve fiber layer; UHR-OCT, ultrahigh-resolution optical coherence tomography.

layers of the horizontal scan (fast scan) and the vertical scan (slow scan) crossing the foveal center, and the thickness map of the total retina were exported and inspected. The six segmented intra-retinal layers were the RNFL, GCIPL, inner nuclear layer (INL), outer plexiform layer (OPL), outer nuclear layer (ONL), and retinal photoreceptor and retinal pigmented epithelium (PR). In addition, total retinal thickness (TRT) was also calculated.

The center of the fovea of all subjects in groups was aligned with the same location before thickness maps were averaged (12,13). The averaged thickness maps were rendered for visualization in Matlab (Ver. 2014b, Mathworks, Natick, MA, USA) (*Figure 1*). Also, ETDRS partition was used to partition the thickness maps into annuli, quadrants, and sectors for further analysis (*Figure 2*). To facilitate the averaging and visualization, the image and dataset of the left eyes were flipped horizontally and averaged with the thickness maps of the right eyes.

Statistical analyses

All data were analyzed with SPSS (Statistical Package for the Social Sciences, Ver. 25, IBM, Armonk, New York, USA). Continuous variables are presented as the mean ± standard deviation (SD). The Kolmogorov-Smirnov test was used to determine whether the variables were normally distributed. Analysis of Covariance (ANCOVA) was used to analyze thickness partitions between age groups with the adjustment of the eye (left and right) and sex. Pearson correlation coefficient, represented by ρ, was used to determine the

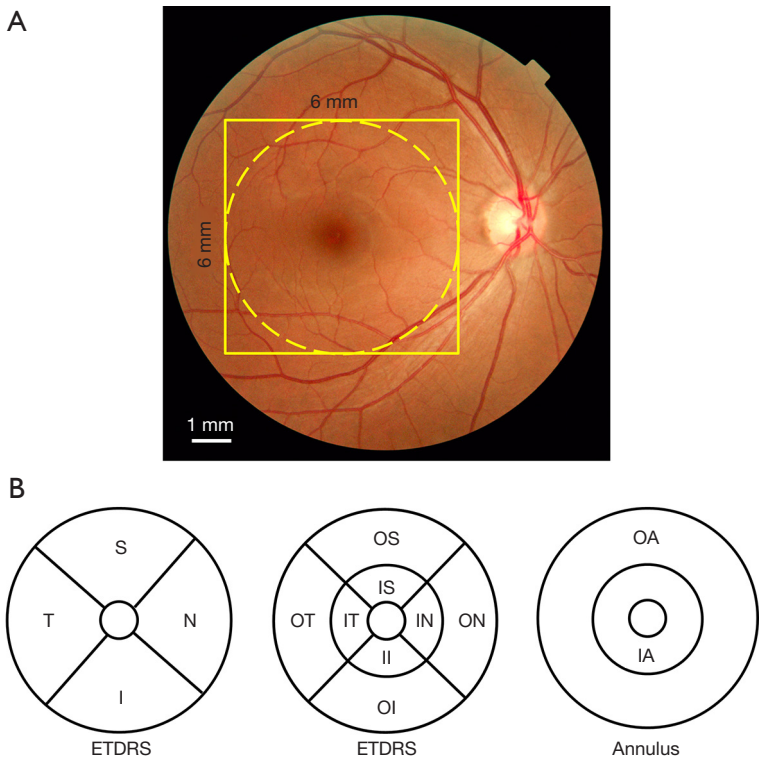

Figure 2 OCT imaging protocols and partition. The macula centered on the fovea was imaged using UHR-OCT, covering an area of 6×6 mm (solid yellow square, A). The dataset was partitioned using the ETDRS partition in quadrants, sectors, and annuli (B). The division by quadrant was performed using 45° and 135° medians (B) with the central 1 mm zone of the fovea removed. Additionally, three concentric rings with diameters of 1, 3, and 6 mm were used to divide the map into nine sectors (B). The inner and outer annuli were also divided (B) using these three concentric rings with diameters of 1, 3, and 6 mm. S, superior; T, temporal; I, inferior; N, nasal; II, inner inferior; IN, inner nasal; IS, inner superior; IT, inferior temporal; OT, outer temporal; OS, outer superior; ON, outer nasal; OI, outer inferior; OA, outer annulus; IA, inner annulus; ETDRS, early treatment of diabetic retinopathy study; OCT, optical coherence tomography; UHR-OCT, ultrahigh-resolution optical coherence tomography.

Table 1 Characteristics of study subjects

Characteristics	G1	G2	G3	G4
Subjects	90	48	33	23
Sex (M:F)	33:57	19:29	11:22	9:14
Age (years)	25.7±4.1	39.9±3.8	56.4±4.0	70.9±5.3

Results are presented as the mean ± SD. Four age groups: G1, <35 years; G2, 35–49 years; G3, 50–64 years; G4 ≥65 years. M, male; F, female; SD, standard deviation.

relations between thickness and age. Linear regression was conducted to identify the slopes of the thickness as a function of age to represent the annual thinning rate. The $P<0.05$ value was considered statistically significant.

Results

Demographics and baseline characteristics of all subjects are showed in *Table 1*.

Intraretinal thickness maps

The average thickness maps showed the alterations among groups, mainly in TRT, mRNFL, and GCIPL (*Figure 3*). By subtracting the thickness map of G1 from other groups, the age-related changes of the thickness maps were visualized in *Figure 4*. The thickness reduction occurred mainly in TRT, mRNFL, GCIPL, INL, and ONL from G2 to G4, compared to G1. Thickness increase was evident in the OPL and PR, mainly in G3 and G4 (*Figure 5*).

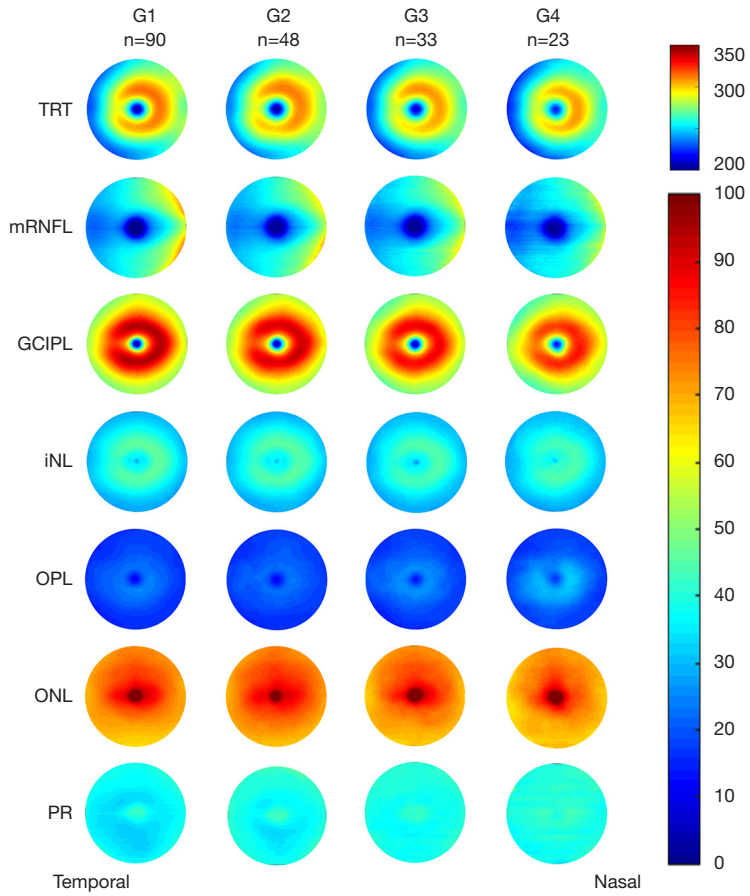

Figure 3 Intraretinal thickness maps. The thickness map of six intraretinal layers was averaged in each group. Four age groups: G1, <35 years; G2, 35–49 years; G3, 50–64 years; G4 ≥65 years. Bar unit: μm. TRT, total retinal thickness; mRNFL, macular retinal nerve fiber layer; GCIPL, ganglion cell-inner plexiform layer; INL, inner nuclear layer; OPL, outer plexiform layer; ONL, outer nuclear layer; PR, retinal photoreceptor.

Focal thinning of the GCIPL

The areas of focal thinning were visualized in elderly eyes (≥65 years), compared to those from other groups in GCIPL (*Figure 6*). The GCIPL thinning pattern in elderly subjects (G4) showed thickness reduction in a round area in the inner annulus around the fovea. The most profound change of the GCIPL was in the inferior sector with an oval zone (length 0.76 mm and width 0.52 mm) 0.61 mm inferior to the fovea, named "A zone". The average thickness reduction of the A zone was 17.15 μm in the elderly group (G4), which was significantly greater than any ETDRS partitions (P<0.05).

The thickness of the intra-retinal layers using the ETDRS partition

All thickness parameters were normally distributed. After the adjustment of eye and sex, annulus analyses (*Figure 7*) showed significant thickness reduction in G4 (P<0.05) in the annulus of the TRT, mRNFL, GCIPL, INL, OPL and ONL, compared to G1 and G2. In addition, there were significant thickness reductions of the annulus in G4 (P<0.05) in TRT, mRNFL, and GCIPL, compared to G3. It was noted that OPL and PR were significantly thicker in G4 in IA, OA and total annulus, compared to G1 (P<0.05).

Analyzed by quadrants (*Figure 8*), there were significant

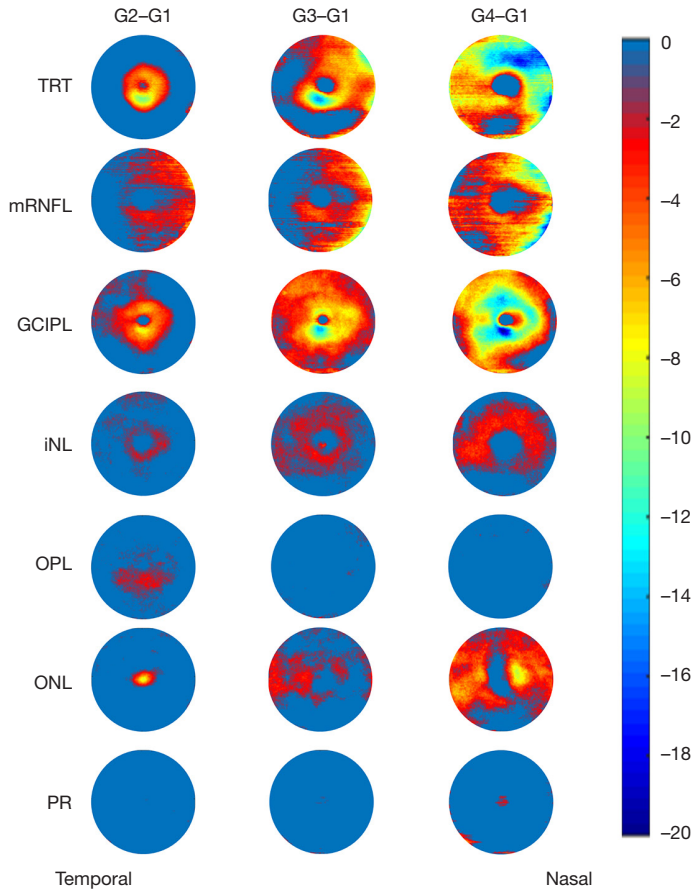

Figure 4 Negative thickness alteration of intraretinal layers. Subtracting the thickness of the young group (G1) from the elder groups (G2–G4), the negative alterations (thickness reduction) were visualized. Thickness reduction mainly occurred in TRT, mRNFL, GCIPL, INL, and ONL in these elder groups. Four age groups: G1, <35 years; G2, 35–49 years; G3, 50–64 years; G4 ≥65 years. Bar unit: μm. TRT, total retinal thickness; mRNFL, macular retinal nerve fiber layer; GCIPL, ganglion cell-inner plexiform layer; INL, inner nuclear layer; OPL, outer plexiform layer; ONL, outer nuclear layer; PR, retinal photoreceptor.

differences of quadrantal (all quadrants) thickness reductions of TRT, mRNFL, GCIPL and INL in G4, compared to G1 ($P<0.05$). In addition, there were significant thickness increases in OPL and PR in some quadrants in G4, compared to G1 ($P<0.05$).

Analyses by eight sectors (*Figure 9*) using the ETDRS partition showed significant thickness reductions ($P<0.05$) in the outer inferior area of TRT, mRNFL, and GCIPL in G4 compared to other groups. There were significant thickness increases in the inner nasal sector of OPL and PR in G4, compared to other groups ($P<0.05$).

Relationship

Age was moderately correlated to the GCIPL thickness of the inner annulus ($\rho=-0.48$; $P<0.001$) and in the A zone ($\rho=-0.39$; $P<0.001$; *Figure 10*). In addition, age was also related to the mRNFL in the outer annulus ($\rho=-0.42$; $P<0.001$) and the annulus ($\rho=-0.44$; $P<0.001$). INL in the inner annulus was also related to age ($\rho=-0.25$; $P<0.05$). In contrast, OPL in the annulus ($\rho=0.33$; $P<0.05$) and PR in the inner annulus ($\rho=0.46$; $P<0.05$) were positively corelated to age.

Annual thinning rate of GCIPL

A linear regression model was used to determine the slopes of the thickness as a function of age to represent the annual thinning rate of GCIPL in different regions (*Figure 11*). The annual thinning rate of GCIPL was the highest in the

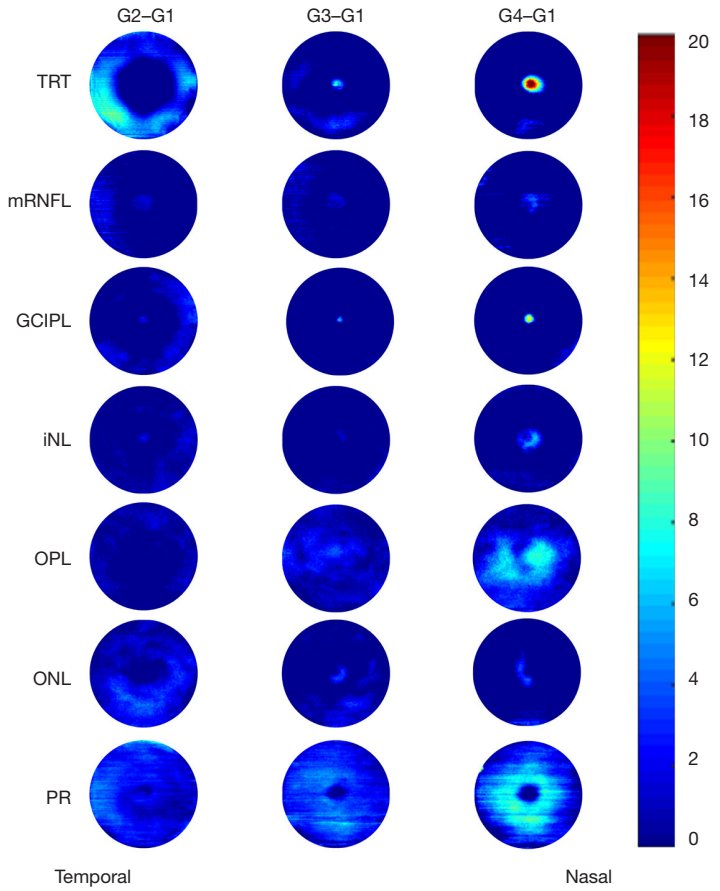

Figure 5 Positive thickness alteration of intraretinal layers. Subtracting the thickness of the young group (G1) from the elder group (G2–G4), the positive alterations (thickness increase) were visualized. Positive changes occurred mainly in OPL and PR in elder groups. Four age groups: G1, <35 years; G2, 35–49 years; G3, 50–64 years; G4 ≥65 years. Bar unit: μm. TRT, total retinal thickness; mRNFL, macular retinal nerve fiber layer; GCIPL, ganglion cell-inner plexiform layer; INL, inner nuclear layer; OPL, outer plexiform layer; ONL, outer nuclear layer; PR, retinal photoreceptor.

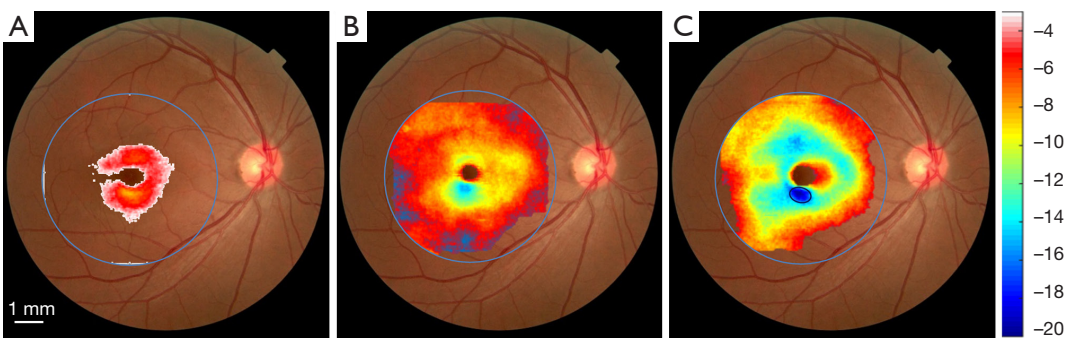

Figure 6 Focal thinning of the GCIPL. The areas of focal thinning of GCIPL showed an increase from G2 (A) then G3 (B) to G4 (C) in the subtraction (subtracted G1) thickness maps. The thinning pattern in elderly subjects (G4) showed thickness reduction in a rounded area in the inner annulus around the fovea. The most profound change of the GCIPL was in the inferior sector with an oval zone (length 0.76 mm and width 0.52 mm) 0.61 mm inferior to the fovea, here named "A zone". Four age groups: G1, <35 years; G2, 35–49 years; G3, 50–64 years; G4 ≥65 years. Bar unit: μm. GCIPL, ganglion cell-inner plexiform layer.

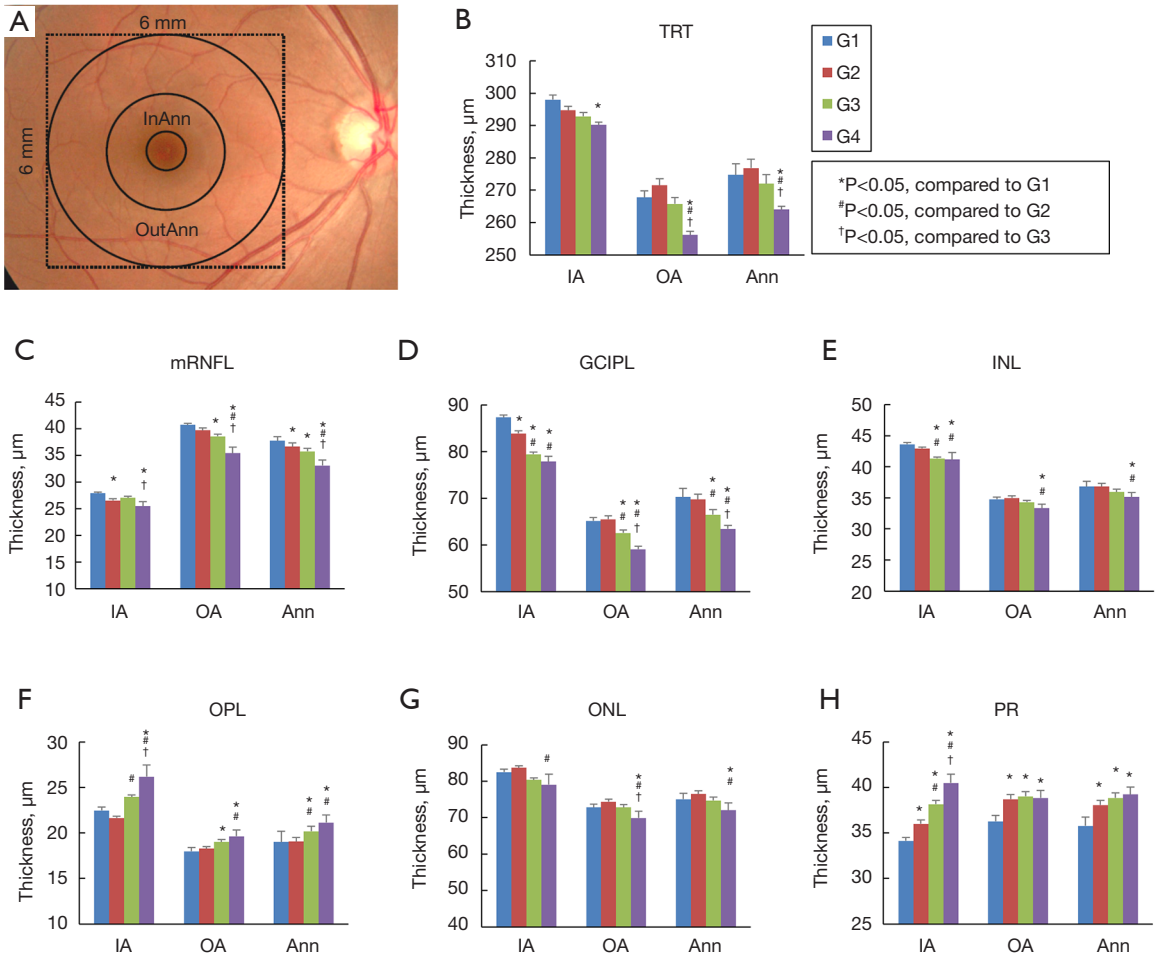

Figure 7 Annular thicknesses of the intraretinal layers. (A) Three concentric rings with diameters of 1, 3, and 6 mm were used to divide the map into annuli. There were significant differences among groups in annular thicknesses of intraretinal layers (B-H). Four age groups: G1, <35 years; G2, 35–49 years; G3, 50–64 years; G4 ≥65 years. Bars = standard error. *, P<0.05, compared to G1; #, P<0.05, compared to G2; †, P<0.05, compared to G3. IA, inner annulus; OA, outer annulus; Ann, total annulus; TRT, total retinal thickness; mRNFL, macular retinal nerve fiber layer; GCIPL, ganglion cell-inner plexiform layer; INL, inner nuclear layer; OPL, outer plexiform layer; ONL, outer nuclear layer; PR, retinal photoreceptor.

A zone (0.33 µm/year, *Figure 11*), followed by the inner inferior sector (0.23 µm/year). The annual thinning rates in the inner sectors (inner inferior, inner nasal and inner superior) were similar to that in the inner annulus.

Discussion

This is the study to apply UHR-OCT for visualizing tomographic intraretinal layer thickness maps in different age groups. We identified the most profound focal alteration of GCIPL in the older 65+ years group. The profound thickness reduction of GCIPL in the inner annulus (1–3 mm in diameter) with a focal region located in the inferior region (i.e., A zone) may represent a characteristic feature of age-related neurodegeneration in the retina. This result may be helpful in further refining the age-related alteration in its location and pattern, which could be used as a normality reference for the diseased conditions. It provides direct visualization of age-related alteration in the GCIPL, which is consistent with previous reports based on pre-set and arbitrary partitions with the averaged results (7,8,10,15).

Our finding that alterations occur in the GCIPL in the inner annulus as part of the aging process is in agreement

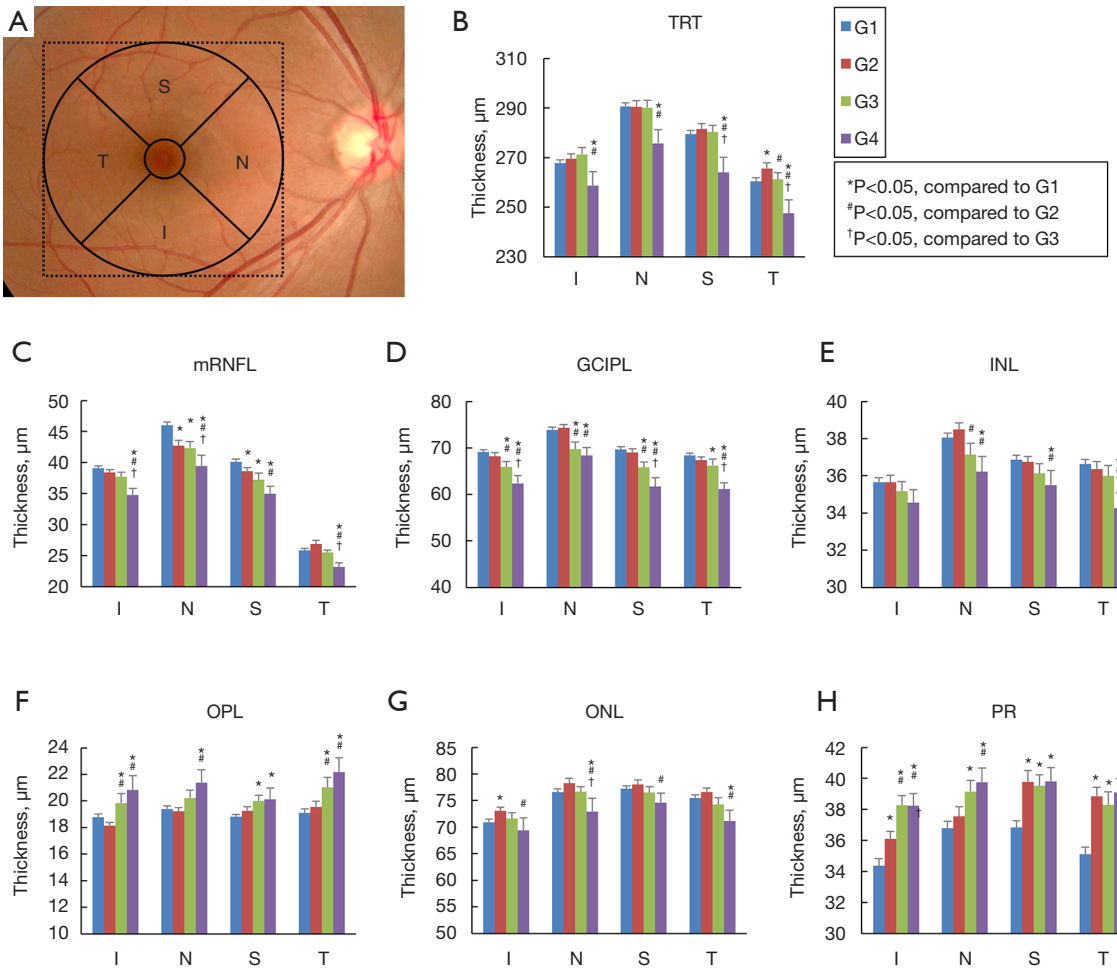

Figure 8 Quadrantal thicknesses of the intraretinal layers. (A) The quadrantal division was obtained using 45° and 135° medians according to the ETDRS partition. There were significant differences among groups in quadrantal thicknesses of intraretinal layers (B-H). Four age groups: G1, <35 years; G2, 35–49 years; G3, 50–64 years; G4 ≥65 years. Bars = standard error. *, P<0.05, compared to G1; #, P<0.05, compared to G2; †, P<0.05, compared to G3. ETDRS, early treatment of diabetic retinopathy study; I, inferior quadrant; N, nasal quadrant; S, superior quadrant; T, temporal quadrant; TRT, total retinal thickness; mRNFL, macular retinal nerve fiber layer; GCIPL, ganglion cell-inner plexiform layer; INL, inner nuclear layer; OPL, outer plexiform layer; ONL, outer nuclear layer; PR, retinal photoreceptor.

with previous studies using ETDRS (8) and Zeiss elliptical partitions (7,10,15). In the study of Yoo *et al.* (8), 573 healthy subjects (5–70 years old) were studied and the study found a significant age-related thinning of the macular ganglion cell layer in the inner annulus, not in the outer annulus of the ETDRS partition. Other studies using the Zeiss elliptical partition (mainly covering the inner annulus) found a thickness reduction during aging in all sectors of the elliptical partition (7,10,15). The thickness reduction may be mainly due to the loss of the neurons and axons in the GCIPL and mRNFL with aging as found in histologic studies of human eyes (16,17).

The thinning rates of the GCIPL found in the present study are also in agreement with previous studies (5,7,18). In the present study, the thinning rates of GCIPL were 0.22, 0.11 and 0.14 μm/year for the inner annulus, outer annulus, and total annulus, respectively. The highest thinning rate was in the inner annulus, which matched the thinning pattern in the thickness maps. Wei *et al.* (5) reported the prominent thinning of 0.21% per year (0.14 μm per year, averaged from 6 mm ETDRS annulus) of GCIPL during 60 years of life. Huo *et al.* (7) reported 0.18 μm per year (averaged from Zeiss elliptical partition) for the average decrease of GCIPL. Longitudinal analyses indicated a

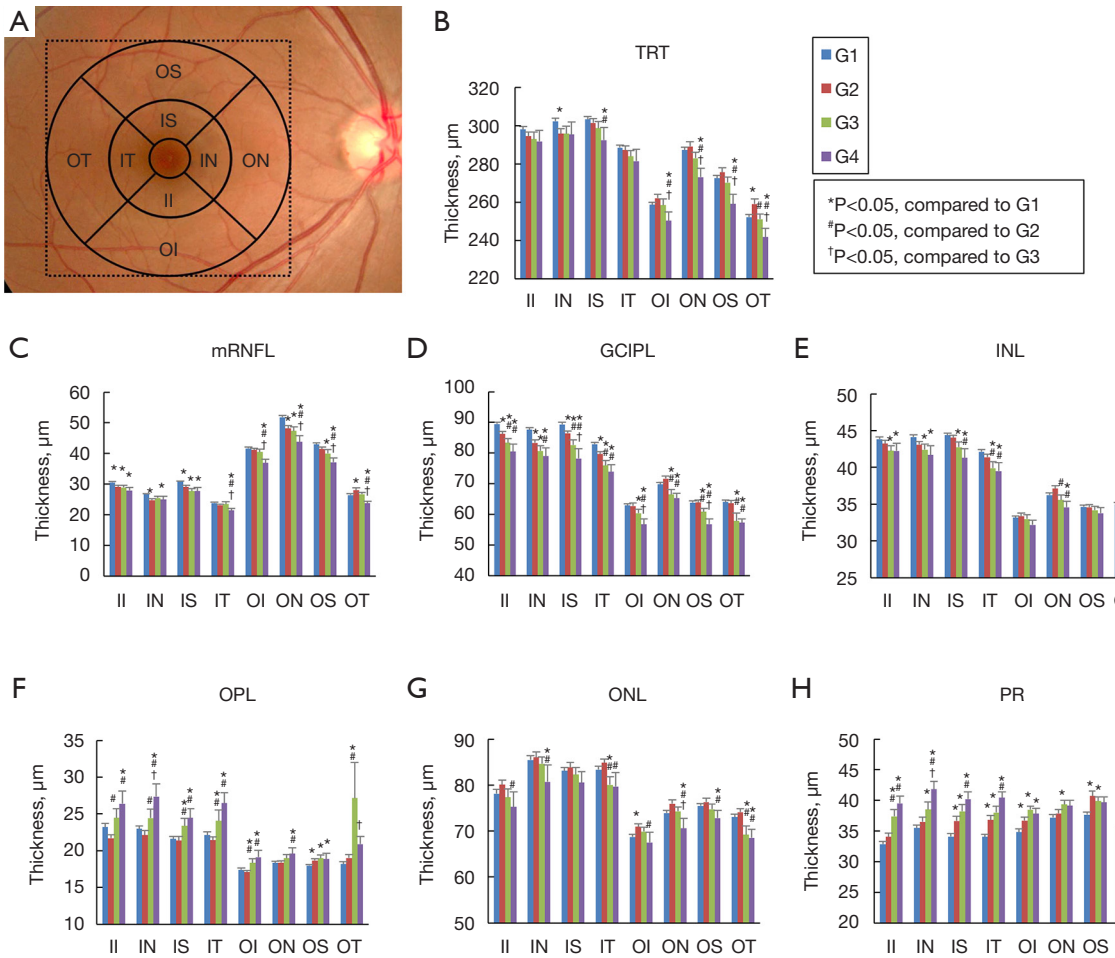

Figure 9 Sectoral thicknesses of the intraretinal layers. (A) According to the ETDRS partition, the quadrantal division was obtained using 45° and 135° medians. Three concentric rings with diameters of 1, 3, and 6 mm were used to divide the map into nine zones. The central 1 mm zone of the fovea was removed. There were significant differences among groups in sectoral thicknesses of intraretinal layers (B-H). Four age groups: G1, <35 years; G2, 35–49 years; G3, 50–64 years; G4 ≥65 years. Bars = standard error. *, P<0.05, compared to G1; #, P<0.05, compared to G2; †, P<0.05, compared to G3. II, inner inferior; IN, inner nasal; IS, inner superior; IT, inferior temporal; OT, outer temporal; OI, outer inferior; ON, outer nasal; OS, outer superior; TRT, total retinal thickness; mRNFL, macular retinal nerve fiber layer; GCIPL, ganglion cell-inner plexiform layer; INL, inner nuclear layer; OPL, outer plexiform layer; ONL, outer nuclear layer; PR, retinal photoreceptor.

thickness decrease of 0.25 μm per year, based on averaged 6-mm diameter thickness map (centered 0.75 mm temporal to the fovea in the combining mRNFL and GCIPL), in subjects over four decades (18). As a reference, the total average rate of ganglion cell loss is reported to be 6 cells/mm^2 per year (17).

While the inner annulus is a relatively large area with the profound thickness reduction during aging, the A zone located in the inferior sector within the inner annulus showed a more profound focal thinning and the highest thinning rate of the GCIPL (0.33 μm per year), compared to any other annuli, quadrants, and sectors. Kim *et al.* (19) analyzed the ganglion cell complex (GCC) in 182 healthy subjects and found that the thinning rate of the inferior GCC was higher than the superior GCC. Huo *et al.* (7) studied 326 healthy Chinese adults and found the highest thinning rates of GCIPL in the inferior nasal and inferior sectors using the elliptical partition. Yoshioka *et al.* (9) used pattern recognition analysis to map the age-related thinning rates of the ganglion cell layer and found that the

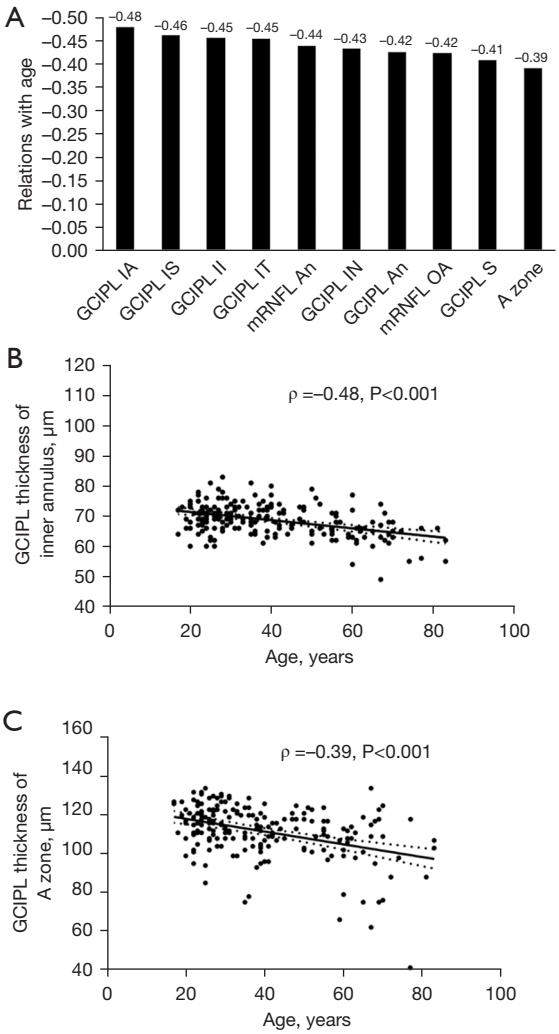

Figure 10 The relations between thicknesses and aging. The top 10 ranked relations with age were the GCIPL and mRNFL including the A zone (A). Scatterplots for the Pearson correlations showed the most correlative sector was the IA of the GCIPL (ρ =−0.48; P<0.001; B). The relation between GCIPL thickness of the A zone was ranked No. 10 (ρ =−0.39; P<0.001; C). ρ, Pearson correlation coefficient. GCIPL, ganglion cell-inner plexiform layer; RNFL, retinal nerve fiber layer; IA, inner annulus; IN, inner nasal; II, inner inferior; IT, inferior temporal; IS, inner superior; An, annulus; OA, outer annulus; S, superior quadrant; mRNFL, macular retinal nerve fiber layer.

highest thinning rate was in the nasal (0.16 μm per year) and inferior (0.14 μm per year) grids (0.9×0.9 mm per grid) within the inner annulus. Koh *et al*. (15) also found that the GCIPL thinning rates over age were equally high in the inferior (0.29 μm per year) and super-nasal sectors (0.29 μm per year) using the elliptical partition. While the mechanism of the location (i.e., A-zone) showing the most significant reduction of GCIPL over aging remains unknown. We noticed that the location of the A-zone is located on the inner inferior sector siting on a horseshoe-like band around the fovea with highest thickness of GCIPL. If the same thinning rate occurs, the highest reduction of the GCIPL could be located in the location with the highest thickness. It could be hypothesized that the A-zone is actually the area with the greatest thickness, resulting in the highest thickness reduction with age, followed by the reduction in the horseshoe-like band. The actual mechanism warrants further investigation.

While the present study and previous studies point to the inferior inner region as the most profound thinning area during aging, the location of the focal thinning zone appeared not to be the same compared to other ocular and systemic diseases (12,20-24). The age-related reduction of retinal cells may be due to mitochondrial dysfunction (25), retrograde neurodegeneration occurring in the cortical regions, as reported in other causes of cortical lesions (26), oxidative stress (27), or retinal and choroidal vascular dysfunction in both large and small vessels associated with age-related macular degeneration-like changes in Bruch's membrane and photoreceptor degeneration (28). Various patterns of retinal ganglion cell (RGC) loss were reported in different disorders (12,20-24). Differentiating the tomographic thinning patterns of the retina may be beneficial when studying ocular, systemic and cerebral neurodegenerative diseases, and their pathophysiology. For instance, the underlying disease process in glaucoma is the loss of RGC (29), and the focal thinning was shown in a particular location of peripapillary RNFL, corresponding to the focal thinning of the macular RGC layer. In patients with glaucoma, the most profound thinning region is found to be in the inferior and temporal regions of the optic disc in RNFL in early stage (30) and a temporal graph sign on the GCIPL thickness map, correlated with visual field loss (31). Also, nasal focal thinning of GCIPL at the pre-symptomatic stage before the diffuse thinning of GCIPL was observed in Leber's hereditary optic neuropathy (LHON). The thinning pattern of GCIPL thickness of LHON followed a centrifugal and spiral pattern in line with the anatomic distribution of the papillomacular bundle fibers (20). Similarly, the most profound thickness reduction zone in multiple sclerosis (MS) was located at the inferonasal sector from the fovea (i.e., M zone) (13)

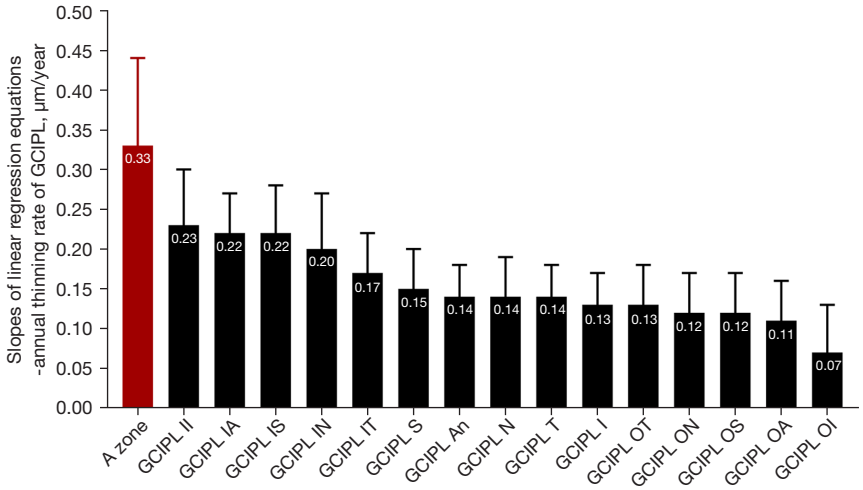

Figure 11 Annual thinning rates of GCIPL. Linear regression analyses showed that the annual thinning rate of GCIPL ranked the highest one was the A zone (0.33 μm/year), followed by the inner inferior sector (0.23 μm/year). The annual thinning rates in the inner sectors (IA, IS and IN) were similar to that in the inner annulus. GCIPL, ganglion cell-inner plexiform layer; II, inner inferior; IA, inner annulus; IS, inner superior; IN, inner nasal; IT, inferior temporal; S, superior quadrant; An, annulus; N, nasal quadrant; T, temporal quadrant; I, inferior quadrant; OT, outer temporal; ON, outer nasal; OS, outer superior; OA, outer annulus; OI, outer inferior.

and resembled the progress of mitochondrial dysfunction, which plays an important pathological role in MS (32). In patients with Alzheimer's disease, the degeneration pattern was shown as GCIPL thinning mainly in the superior region (12). Considering the results in the present study and previous studies showing the thickness alteration patterns, detailed analysis using the ETDRS partitions may be preferable.

As expected, significantly generalized thickness reduction of mRNFL paralleled the generalized GCIPL loss with aging in the oldest group compared to other groups, all of whom were less than 65 years. Similarly, the coordinate reduction of both GCIPL and mRNFL in a centrifugal and spiral pattern were reported in LHON (20), generalized reduction in retinitis pigmentosa (33), and sectoral loss branch retinal vein occlusion (34). However, the outer temporal regional GCIPL thickness reduction and outer inferior and outer nasal mRNFL accession are reported in papilledema eyes (35).

The thinning of INL and ONL found in the present study is consistent with histopathological results demonstrating nuclei displacement from INL and ONL into OPL as a function of age (36). Of note, Henle fiber layer is within the OPL, which may contribute to the changes. However, we did not differentiate the Henle fiber layer from the OPL in the present study. Other than the cell translocation, the increased OPL may also be due to the accumulation of discs of outer segments and waste products. Interestingly, the ONL thickness in the fovea appeared to be preserved, which echoes the previous observation (37). Similar findings were seen in patients with early and intermediate age-related macular degeneration (38). In contrast, increased thickness of INL due to inflammation is reported in patients with MS (39). The thickening of retinal pigment epithelium (RPE) has been reported by histologic studies (40,41), and might be due to the accumulation of discs of outer segments, various kinds of secretory as well as waste products in and around the RPE or possibly related local inflammation (41). It may also be due to accumulating of lipofuscin, resulted from lysosomal dysfunction (42). Meanwhile, the atrophy of photoreceptor cells is found in elderly people (43) may also contribute to their vision loss. In the present study, PR (including both RPE and photoreceptor layers) were found to be significantly thicker in elder groups. This could be explained by the accumulation of lipofuscin during aging are more obvious than the atrophy of photoreceptor cells.

There are several limitations to our study. First, we have fewer subjects who were 65 years of age and older. A greater number of elderly individuals would have strengthened our findings with regard to thickness map alterations. Second, we analyzed 6 mm region of the macula, but did

not analyze the peripapillary region. However, the macula area represented a good collection of axons arising from RGCs and has a good correlation with the peripapillary retina in terms of thickness changes (43). Third, we did not follow-up on these subjects as this was a cross-sectional study. In longitudinal and cross-sectional analyses, Zhang *et al*. (18) found consistent rates of age-related thinning in GCC thickness. Lastly, the present study focused on the visualization of the age-related alteration of intraretinal layers. We found that the profound thickness change of GCIPL was related to age. Further studies need to address whether such changes in thickness have any impact on vision are needed.

In conclusion, this is the study to apply UHR-OCT for visualizing the age-related alteration of intraretinal layers in a general population. The most profound change of the optic nerve fiber is an oval-like focal thinning in GCIPL, which occurred in the inferior sector within the inner annulus. This finding may be used as a reference for normal age-related peripheral neurodegeneration patterns in future studies.

Acknowledgments

Funding: The work was supported by the Evelyn F. McKnight Brain Institute, National Institute of Health Center Grant P30 EY014801, National Institute of Health NINDS 1R01NS111115-01 (JW), a grant from Research to Prevent Blindness (RPB). Scholarly activities of YD were supported by the National Natural Science Foundation of China (82171015) in Zhongshan Ophthalmic Center, Sun Yat-sen University, Guangzhou, China. Scholarly activities of JZ were supported by grants from Wenzhou Science and Technology Bureau (G20190023) and Natural Science Foundation of Zhejiang Province (Q17H180019).

Footnote

Reporting Checklist: The authors have completed the STROBE reporting checklist. Available at https://qims.amegroups.com/article/view/10.21037/qims-21-860/rc

Conflicts of Interest: All authors have completed the ICMJE uniform disclosure form (available at https://qims.amegroups.com/article/view/10.21037/qims-21-860/coif). The authors have no conflicts of interest to declare.

Ethical Statement: The authors are accountable for all aspects of the work in ensuring that questions related to the accuracy or integrity of any part of the work are appropriately investigated and resolved. The study was conducted in accordance with the Declaration of Helsinki (as revised in 2013) and approved by the Institutional Review Board of the University of Miami. All subjects were recruited voluntarily and were informed about the purposes, methods, and the potential risks of the study. A signed consent form was obtained from each volunteer.

References

1. Ramanan VK, Saykin AJ. Pathways to neurodegeneration: mechanistic insights from GWAS in Alzheimer's disease, Parkinson's disease, and related disorders. Am J Neurodegener Dis 2013;2:145-75.
2. Wang JT, Medress ZA, Barres BA. Axon degeneration: molecular mechanisms of a self-destruction pathway. J Cell Biol 2012;196:7-18.
3. Alamouti B, Funk J. Retinal thickness decreases with age: an OCT study. Br J Ophthalmol 2003;87:899-901.
4. Iverson SM, Feuer WJ, Shi W, Greenfield DS; Advanced Imaging for Glaucoma Study Group. Frequency of abnormal retinal nerve fibre layer and ganglion cell layer SDOCT scans in healthy eyes and glaucoma suspects in a prospective longitudinal study. Br J Ophthalmol 2014;98:920-5.
5. Wei Y, Jiang H, Shi Y, Qu D, Gregori G, Zheng F, Rundek T, Wang J. Age-Related Alterations in the Retinal Microvasculature, Microcirculation, and Microstructure. Invest Ophthalmol Vis Sci 2017;58:3804-17.
6. Hammel N, Belghith A, Weinreb RN, Medeiros FA, Mendoza N, Zangwill LM. Comparing the Rates of Retinal Nerve Fiber Layer and Ganglion Cell-Inner Plexiform Layer Loss in Healthy Eyes and in Glaucoma Eyes. Am J Ophthalmol 2017;178:38-50.
7. Huo YJ, Guo Y, Li L, Wang HZ, Wang YX, Thomas R, Wang NL. Age-related changes in and determinants of

macular ganglion cell-inner plexiform layer thickness in normal Chinese adults. Clin Exp Ophthalmol 2018;46:400-6.
8. Yoo YJ, Hwang JM, Yang HK. Inner macular layer thickness by spectral domain optical coherence tomography in children and adults: a hospital-based study. Br J Ophthalmol 2019;103:1576-83.
9. Yoshioka N, Zangerl B, Nivison-Smith L, Khuu SK, Jones BW, Pfeiffer RL, Marc RE, Kalloniatis M. Pattern Recognition Analysis of Age-Related Retinal Ganglion Cell Signatures in the Human Eye. Invest Ophthalmol Vis Sci 2017;58:3086-99.
10. Mwanza JC, Durbin MK, Budenz DL, Girkin CA, Leung CK, Liebmann JM, Peace JH, Werner JS, Wollstein G; Cirrus OCT Normative Database Study Group. Profile and predictors of normal ganglion cell-inner plexiform layer thickness measured with frequency-domain optical coherence tomography. Invest Ophthalmol Vis Sci 2011;52:7872-9.
11. Lin Y, Jiang H, Liu Y, Rosa Gameiro G, Gregori G, Dong C, Rundek T, Wang J. Age-Related Alterations in Retinal Tissue Perfusion and Volumetric Vessel Density. Invest Ophthalmol Vis Sci 2019;60:685-93.
12. Shao Y, Jiang H, Wei Y, Shi Y, Shi C, Wright CB, Sun X, Vanner EA, Rodriguez AD, Lam BL, Rundek T, Baumel BS, Gameiro GR, Dong C, Wang J. Visualization of Focal Thinning of the Ganglion Cell-Inner Plexiform Layer in Patients with Mild Cognitive Impairment and Alzheimer's Disease. J Alzheimers Dis 2018;64:1261-73.
13. Shi C, Jiang H, Gameiro GR, Hu H, Hernandez J, Delgado S, Wang J. Visual Function and Disability Are Associated With Focal Thickness Reduction of the Ganglion Cell-Inner Plexiform Layer in Patients With Multiple Sclerosis. Invest Ophthalmol Vis Sci 2019;60:1213-23.
14. Tan J, Yang Y, Jiang H, Liu C, Deng Z, Lam BL, Hu L, Oakley J, Wang J. The measurement repeatability using different partition methods of intraretinal tomographic thickness maps in healthy human subjects. Clin Ophthalmol 2016;10:2403-15.
15. Koh VT, Tham YC, Cheung CY, Wong WL, Baskaran M, Saw SM, Wong TY, Aung T. Determinants of ganglion cell-inner plexiform layer thickness measured by high-definition optical coherence tomography. Invest Ophthalmol Vis Sci 2012;53:5853-9.
16. Harman A, Abrahams B, Moore S, Hoskins R. Neuronal density in the human retinal ganglion cell layer from 16-77 years. Anat Rec 2000;260:124-31.
17. Gao H, Hollyfield JG. Aging of the human retina. Differential loss of neurons and retinal pigment epithelial cells. Invest Ophthalmol Vis Sci 1992;33:1-17.
18. Zhang X, Francis BA, Dastiridou A, Chopra V, Tan O, Varma R, Greenfield DS, Schuman JS, Huang D; Advanced Imaging for Glaucoma Study Group. Longitudinal and Cross-Sectional Analyses of Age Effects on Retinal Nerve Fiber Layer and Ganglion Cell Complex Thickness by Fourier-Domain OCT. Transl Vis Sci Technol 2016;5:1.
19. Kim NR, Kim JH, Lee J, Lee ES, Seong GJ, Kim CY. Determinants of perimacular inner retinal layer thickness in normal eyes measured by Fourier-domain optical coherence tomography. Invest Ophthalmol Vis Sci 2011;52:3413-8.
20. Balducci N, Savini G, Cascavilla ML, La Morgia C, Triolo G, Giglio R, Carbonelli M, Parisi V, Sadun AA, Bandello F, Carelli V, Barboni P. Macular nerve fibre and ganglion cell layer changes in acute Leber's hereditary optic neuropathy. Br J Ophthalmol 2016;100:1232-7.
21. Carelli V, La Morgia C, Sadun AA. Mitochondrial dysfunction in optic neuropathies: animal models and therapeutic options. Curr Opin Neurol 2013;26:52-8.
22. Shin JW, Sung KR, Park SW. Patterns of Progressive Ganglion Cell-Inner Plexiform Layer Thinning in Glaucoma Detected by OCT. Ophthalmology 2018;125:1515-25.
23. La Morgia C, Ross-Cisneros FN, Sadun AA, Carelli V. Retinal Ganglion Cells and Circadian Rhythms in Alzheimer's Disease, Parkinson's Disease, and Beyond. Front Neurol 2017;8:162.
24. La Morgia C, Di Vito L, Carelli V, Carbonelli M. Patterns of Retinal Ganglion Cell Damage in Neurodegenerative Disorders: Parvocellular vs Magnocellular Degeneration in Optical Coherence Tomography Studies. Front Neurol 2017;8:710.
25. Fudalej E, Justyniarska M, Kasarełło K, Dziedziak J, Szaflik JP, Cudnoch-Jędrzejewska A. Neuroprotective Factors of the Retina and Their Role in Promoting Survival of Retinal Ganglion Cells: A Review. Ophthalmic Res 2021;64:345-55.
26. Prasad T, Zhu P, Verma A, Chakrabarty P, Rosario AM, Golde TE, Li Q. Amyloid β peptides overexpression in retinal pigment epithelial cells via AAV-mediated gene transfer mimics AMD-like pathology in mice. Sci Rep 2017;7:3222.
27. Bonilha VL, Bell BA, Rayborn ME, Samuels IS, King A, Hollyfield JG, Xie C, Cai H. Absence of DJ-1 causes age-related retinal abnormalities in association with increased

oxidative stress. Free Radic Biol Med 2017;104:226-37.
28. Johnson MA, Lutty GA, McLeod DS, Otsuji T, Flower RW, Sandagar G, Alexander T, Steidl SM, Hansen BC. Ocular structure and function in an aged monkey with spontaneous diabetes mellitus. Exp Eye Res 2005;80:37-42.
29. Nickells RW. From ocular hypertension to ganglion cell death: a theoretical sequence of events leading to glaucoma. Can J Ophthalmol 2007;42:278-87.
30. Le PV, Tan O, Chopra V, Francis BA, Ragab O, Varma R, Huang D. Regional correlation among ganglion cell complex, nerve fiber layer, and visual field loss in glaucoma. Invest Ophthalmol Vis Sci 2013;54:4287-95.
31. Lee J, Kim YK, Ha A, Kim YW, Baek SU, Kim JS, Lee HJ, Kim DW, Jeoung JW, Kim SJ, Park KH. Temporal Raphe Sign for Discrimination of Glaucoma from Optic Neuropathy in Eyes with Macular Ganglion Cell-Inner Plexiform Layer Thinning. Ophthalmology 2019;126:1131-9.
32. Dutta R, McDonough J, Yin X, Peterson J, Chang A, Torres T, Gudz T, Macklin WB, Lewis DA, Fox RJ, Rudick R, Mirnics K, Trapp BD. Mitochondrial dysfunction as a cause of axonal degeneration in multiple sclerosis patients. Ann Neurol 2006;59:478-89.
33. Alshareef RA, You Q, Barteselli G, Rao HL, Goud A, Chhablani J. In Vivo Evidence of Inner Retinal Neurodegeneration in Retinitis Pigmentosa Using Spectral-Domain Optical Coherence Tomography. Ophthalmic Surg Lasers Imaging Retina 2016;47:828-35.
34. Alshareef RA, Barteselli G, You Q, Goud A, Jabeen A, Rao HL, Jabeen A, Chhablani J. In vivo evaluation of retinal ganglion cells degeneration in eyes with branch retinal vein occlusion. Br J Ophthalmol 2016;100:1506-10.
35. Aghsaei Fard M, Okhravi S, Moghimi S, Subramanian PS. Optic Nerve Head and Macular Optical Coherence Tomography Measurements in Papilledema Compared With Pseudopapilledema. J Neuroophthalmol 2019;39:28-34.
36. Gartner S, Henkind P. Aging and degeneration of the human macula. 1. Outer nuclear layer and photoreceptors. Br J Ophthalmol 1981;65:23-8.
37. Etheridge T, Liu Z, Nalbandyan M, Cleland S, Blodi BA, Mares JA, Bailey S, Wallace R, Gehrs K, Tinker LF, Gangnon R, Domalpally A; CAREDS2 Research Study Group. Association of Macular Thickness With Age and Age-Related Macular Degeneration in the Carotenoids in Age-Related Eye Disease Study 2 (CAREDS2), An Ancillary Study of the Women's Health Initiative. Transl Vis Sci Technol 2021;10:39.
38. Lamin A, Oakley JD, Dubis AM, Russakoff DB, Sivaprasad S. Changes in volume of various retinal layers over time in early and intermediate age-related macular degeneration. Eye (Lond) 2019;33:428-34.
39. Saidha S, Sotirchos ES, Ibrahim MA, Crainiceanu CM, Gelfand JM, Sepah YJ, Ratchford JN, Oh J, Seigo MA, Newsome SD, Balcer LJ, Frohman EM, Green AJ, Nguyen QD, Calabresi PA. Microcystic macular oedema, thickness of the inner nuclear layer of the retina, and disease characteristics in multiple sclerosis: a retrospective study. Lancet Neurol 2012;11:963-72.
40. Nag TC, Wadhwa S. Ultrastructure of the human retina in aging and various pathological states. Micron 2012;43:759-81.
41. Anderson DH, Mullins RF, Hageman GS, Johnson LV. A role for local inflammation in the formation of drusen in the aging eye. Am J Ophthalmol 2002;134:411-31.
42. Sparrow JR, Boulton M. RPE lipofuscin and its role in retinal pathobiology. Exp Eye Res 2005;80:595-606.
43. Garvin MK, Abràmoff MD, Lee K, Niemeijer M, Sonka M, Kwon YH. 2-D pattern of nerve fiber bundles in glaucoma emerging from spectral-domain optical coherence tomography. Invest Ophthalmol Vis Sci 2012;53:483-9.

Cite this article as: Deng Y, Wang H, Simms AG, Hu H, Zhang J, Gameiro GR, Rundek T, Signorile JF, Levin BE, Yuan J, Wang J, Jiang H. Age-related focal thinning of the ganglion cell-inner plexiform layer in a healthy population. Quant Imaging Med Surg 2022;12(6):3034-3048. doi: 10.21037/qims-21-860

